Cell

Actin Dynamics Drive Membrane Reorganization and Scission in Clathrin-Independent Endocytosis

Winfried Römer,[1,*] Léa-Laetitia Pontani,[2] Benoît Sorre,[3,4] Carles Rentero,[5] Ludwig Berland,[3] Valérie Chambon,[1] Christophe Lamaze,[1] Patricia Bassereau,[3] Cécile Sykes,[2] Katharina Gaus,[5] and Ludger Johannes[1,*]
[1]Institut Curie, Centre de Recherche, Traffic, Signaling and Delivery group, CNRS UMR 144
[2]Institut Curie, Centre de Recherche, Biomimetism of Cell Movement group, CNRS UMR 168, Physico-Chimie Curie, Université Pierre et Marie Curie
[3]Institut Curie, Centre de Recherche, Membrane and Cell Functions group, CNRS UMR 168, Physico-Chimie Curie, Université Pierre et Marie Curie
[4]Institut Curie, Centre de Recherche, Molecular Mechanisms of Intracellular Transport group, CNRS UMR 144
26 rue d'Ulm, 75248 Paris Cedex 05, France
[5]Centre for Vascular Research, University of New South Wales, Sydney, and the Department of Haematology, Prince of Wales Hospital, Sydney, New South Wales 2052, Australia
*Correspondence: winfried.roemer@curie.fr (W.R.), johannes@curie.fr (L.J.)
DOI 10.1016/j.cell.2010.01.010

SUMMARY

Nascent transport intermediates detach from donor membranes by scission. This process can take place in the absence of dynamin, notably in clathrin-independent endocytosis, by mechanisms that are yet poorly defined. We show here that in cells scission of Shiga toxin-induced tubular endocytic membrane invaginations is preceded by cholesterol-dependent membrane reorganization and correlates with the formation of membrane domains on model membranes, suggesting that domain boundary forces are driving tubule membrane constriction. Actin triggers scission by inducing such membrane reorganization process. Tubule occurrence is indeed increased upon cellular depletion of the actin nucleator component Arp2, and the formation of a cortical actin shell in liposomes is sufficient to trigger the scission of Shiga toxin-induced tubules in a cholesterol-dependent but dynamin-independent manner. Our study suggests that membranes in tubular Shiga toxin-induced invaginations are poised to undergo actin-triggered reorganization leading to scission by a physical mechanism that may function independently from or in synergy with pinchase activity.

INTRODUCTION

Intracellular trafficking of proteins and lipids involves a sequence of events in which the scission of nascent transport intermediates from the donor membrane is one of the key steps (Bonifacino and Glick, 2004). Because of its central role in many trafficking events, dynamin has become a paradigm for studying the process of membrane scission (reviewed in Mettlen et al., 2009; Praefcke and McMahon, 2004). Yet, compelling evidence exists that in some instances the scission process can also occur in a dynamin-independent manner. The dynamin homologs in the budding yeast *Saccharomyces cerevisiae* are not involved in scission, and in flies, acute perturbation of dynamin function has revealed that not all endocytic processes require this GTPase (Guha et al., 2003). How plasma membrane invaginations can undergo scission without dynamin remains largely unexplored at this stage.

Several of the clathrin-independent endocytosis pathways in more complex eukaryotes also do not involve dynamin. Examples are the CLIC/GEEC pathway for the cellular uptake of GPI-anchored proteins (reviewed in Kirkham and Parton, 2005; Mayor and Pagano, 2007) and the uptake of simian virus 40 in the absence of caveolae (Damm et al., 2005). One aspect that is common to these endocytic processes is their sensitivity to cholesterol and the involvement of glycosphingolipids. Although it has already been well established that glycosphingolipids are the cellular receptors of simian virus 40 and other polyoma viruses (Tsai et al., 2003), it remains to be determined how exactly these classes of lipids regulate GPI-anchored protein trafficking in a process that involves cholesterol-sensitive nanodomains (Sharma et al., 2004) and their active clustering as a consequence of actin dynamics (Goswami et al., 2008).

Glycosphingolipids are also cellular receptors for protein toxins. One well-studied example is the bacterial Shiga toxin, produced by *Shigella dysenteriae* and by enterohemorrhagic strains of *Escherichia coli*. Via its homopentameric B-subunit, Shiga toxin binds to the glycosphingolipid Gb3. Shiga toxin enters cells efficiently even when the function of clathrin is inhibited (Lauvrak et al., 2004; Saint-Pol et al., 2004). After endocytosis, Shiga toxin leaves the endocytic pathway at the level of early endosomes (Mallard et al., 1998) and is then transported to the Golgi apparatus and the endoplasmic reticulum (Sandvig et al., 1992), following the retrograde transport route (reviewed

in Bonifacino and Rojas, 2006; Johannes and Popoff, 2008). From the lumen of the endoplasmic reticulum, the catalytic A-subunit is translocated to the cytosol to reach its molecular target, ribosomal RNA, whose toxin-mediated modification leads to the inhibition of protein biosynthesis.

Our previous studies have shown that the receptor-binding nontoxic B-subunit of Shiga toxin (STxB) induces endocytic plasma membrane invaginations (Römer et al., 2007). These negative membrane curvature changes are driven by compaction of glycosphingolipid receptors under the STxB protein (Windschiegl et al., 2009), leading to transbilayer torque and spontaneous membrane bending toward the toxin (Sens et al., 2008). Active cellular machinery is required for tubule processing, not for formation. Dynamin binds to these tubular invaginations, and, when functionally inhibited, an increased occurrence of plasma membrane-connected STxB-containing tubules is observed, thus suggesting that dynamin contributes to their scission. Scission is also dependent on plasma membrane cholesterol levels (Römer et al., 2007), pointing at specific lipid composition requirements.

In the current work, we have investigated scission of STxB-induced tubules on cell and model membranes. Scission can be spontaneously triggered and tightly correlates with membrane reorganization and membrane domain formation. Actin is localized on STxB-induced invaginations, and interfering with actin dynamics prevents their scission, which is paralleled by an absence of membrane reorganization. In a model membrane system we found that the formation of a cortical actin shell leads to the cholesterol-dependent scission of STxB-induced invaginations, even in the absence of dynamin. Based on these findings, we propose a model in which actin triggers the reorganization of tubular membrane invaginations leading to scission. Here, the squeezing of the tubular structure results from the physical pinching produced by membrane in order to reduce the contact between domains, and not from pinchase activity of GTPases.

RESULTS

Temperature Shift Induces Cholesterol-Dependent Membrane Reorganization and Scission

In a previous study we have shown that STxB induces the formation of tubular endocytic invaginations, whose scission depends on cholesterol levels, suggesting that specific membrane states are of critical importance (Römer et al., 2007). To further investigate this process, cells with STxB-induced tubules were shifted to lower temperatures in order to favor domain formation. The underlying rational was that tubule stability would depend on temperature if it involved membrane reorganization at scales larger than molecular, such as when domain formation is induced.

Conditions were chosen in which cells have many STxB-induced tubular invaginations (Römer et al., 2007), which is the case upon inhibition of (1) actin polymerization, using latrunculin A or by depletion of actin nucleator complex component Arp2 (Figures S1A and S1B available online); (2) dynamin, using the small-molecule inhibitor dynasore (Macia et al., 2006) (Figure S1C); (3) active cellular machinery, using an established protocol for energy depletion (Figure 1A). In all these conditions, tubule morphologies were well preserved when the cells were fixed at 37°C. In contrast, when fixation was done at 19.5°C (Figure 1B) or 4°C (Figure 1C and Figures S1A–S1C), tubular structures were rarely detected, suggesting that STxB-induced invaginations underwent scission.

The hypothesis of temperature shift-induced scission was quantitatively analyzed by coupling biotin to STxB via a cleavable disulphide bond so that intracellular pools of STxB can be measured by their inaccessibility to a membrane-impermeable reducing agent, MESNA (Amessou et al., 2006). Energy-depleted cells were incubated with biotinylated STxB at 37°C to induce tubule formation (Figure 1D, black bars), and cell-surface inaccessibility was then analyzed at 37°C, 19.5°C, and 4°C (as indicated on the x axis). Background was determined by primary incubation at 4°C (Figure 1D, open bars) when STxB does not induce tubules (Römer et al., 2007). When cells were left at 37°C, all biotinylated STxB was cleaved by the reducing agent (Figure 1D), demonstrating that the tubular structures observed under these conditions (Figure 1A) were still connected to the cell surface. In contrast, upon shift to 19.5°C or 4°C, a sizable fraction of biotinylated STxB became cell surface inaccessible (Figure 1D, black bars). These data established that tubule scission could be induced by temperature shift. A time-resolved analysis of these findings including morphological and biochemical controls of cell-surface inaccessibility can be found in the Supplemental Information (Figures S2A–S2G). Furthermore, the biochemical cell-surface inaccessibility assay showed that STxB-containing tubules were also disconnected from the cell surface in dynasore-treated cells upon shift to low temperatures (Figure S2H).

Our finding that the scission of STxB-induced invaginations can be triggered by temperature shift in different conditions, including cells in which active cellular machinery was inhibited, confirmed our initial hypothesis that tubule integrity was selectively dependent on specific membrane states, a point that we further explored.

First, cholesterol has key functions in stabilizing lipid assemblies (Simons and Vaz, 2004) and regulates domain formation (Bacia et al., 2005) such that varying cholesterol levels can determine whether a lipid system is homogenous or phase separated (McConnell and Vrljic, 2003). After extracting plasma membrane cholesterol, STxB could still induce tubular invaginations (Figure 1E), as reported previously (Römer et al., 2007), but strikingly, a temperature shift from 37°C to as low as 4°C did not affect tubule integrity (Figure 1F), in sharp contrast to the situation described above for cells with normal cholesterol levels (Figure 1A versus Figure 1C). Biochemical analysis confirmed that STxB remained cell surface accessible on energy-depleted (Figure 1G) and control (Figure 1H) cells that were cholesterol extracted, even after a shift to 4°C.

In a second series of experiments, we used the polarity-sensitive membrane dye Laurdan in combination with two-photon laser-scanning microscopy (Gaus et al., 2003; Römer et al., 2007) to analyze changes in membrane organization of tubular invaginations that undergo temperature shift-induced scission. Membrane order is characterized by general-polarization (GP) values, which are pseudocolored in Figure 2B.

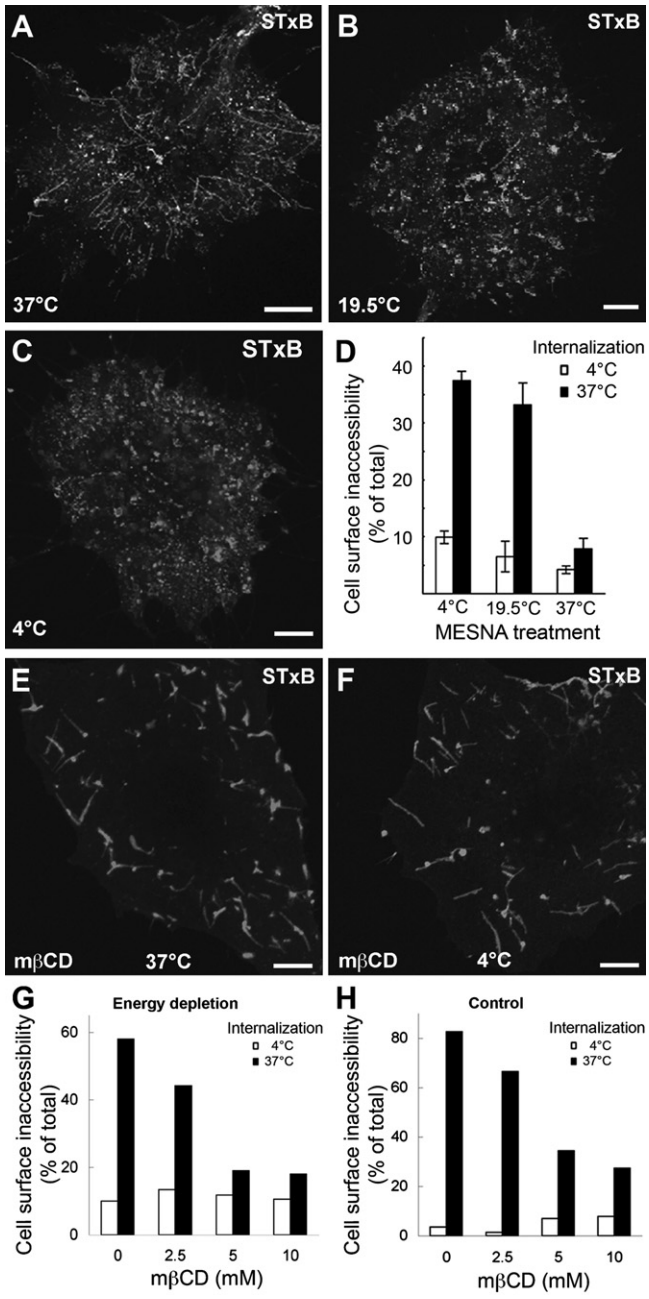

Figure 1. Temperature Shift Triggers Scission of STxB-Induced Tubular Membrane Invaginations

(A–C) Energy-depleted HeLa cells with STxB-induced tubules were fixed with 4% PFA at 37°C (A), 19.5°C (B), or 4°C (C). Tubules were lost upon incubations at temperatures below 37°C.

(D) Biotin-tagged STxB was incubated for 40 min at 4°C (open bars) or 37°C (black bars) with energy-depleted cells. The cells were then treated at temperatures indicated on the x axis (4°C, 19.5°C, 37°C) with membrane-impermeable MESNA that cleaves the biotin tag off STxB. Note that upon temperature shift below 37°C, a fraction of STxB becomes cell surface inaccessible. Means ± standard error of the mean (SEM) of three experiments.

(E and F) Energy-depleted and cholesterol-extracted HeLa cells with STxB-induced tubules were fixed at 37°C (E) or 4°C (F). After cholesterol extraction, temperature shift does not induce tubule scission any more.

Energy-depleted cells were concomitantly imaged for STxB (Figure 2A, red) while the temperature of the media dropped slowly from 35°C to 23°C. We observed that tubule integrity was preserved until 26°C (Figure 2A). In contrast, GP values had already decreased at this point (Figure 2B), demonstrating that changes in membrane organization preceded the scission event. Indeed, a comparison between STxB intensity and GP profile along the membrane tubule shows that the STxB tubule was essentially unaltered when temperature was lowered from 35°C to 29°C (Figure S3B), whereas the membrane was reorganized during temperature shift (Figure S3C).

When quantified over many cells, we confirmed that STxB-positive membrane structures indeed had significantly lower GP values when fixed at 19.5°C or 4°C, compared to those fixed at 37°C (Figure 2C). Strikingly, under cholesterol extraction conditions, where temperature shift did not lead to tubule scission (Figures 1E–1H), shifts to lower temperature did not result in a significant decrease in the GP value of tubular STxB membranes (Figure 2C, mßCD), demonstrating a tight correlation between changes in membrane organization and subsequent scission.

Domain Formation Correlates with Scission of STxB-Induced Tubules

The fact that scission of tubular endocytic membrane invaginations could be triggered by temperature shift in a cholesterol-dependent manner under conditions where active cellular machinery was inhibited indicated that the process could be a physical property of the STxB-induced membrane environment. To test this prediction directly, we reconstituted the process in a model membrane system. We chose giant unilamellar vesicles (GUVs) on which STxB drives the formation of tubular membrane invaginations with morphologies similar to those seen on cells (Römer et al., 2007). GUVs were prepared with or without cholesterol at 30 mol% using 1,2-dioleoylphosphatidyl choline (DOPC) and Gb3 that was purified from HeLa cells (5 mol%) (Figure 3). Cy3-labeled STxB (red) bound to GUVs (spiked with Bodipy$_{FL}$-C$_5$-HPC, green) and induced tubular membrane invaginations. Prolonged incubation at 37°C for hours had no visible effect on tubule integrity, independently of cholesterol content of the GUVs (Figures 3A and 3B). When GUVs that did not contain cholesterol were shifted to 4°C, tubule integrity was not affected (Figure 3D). In contrast, temperature shift to 4°C of GUVs containing cholesterol led to tubule scission and the accumulation of membrane fragments in the GUV lumen (Figure 3C). Quantification showed that intralumenal fluorescence was indeed selectively increased in this condition (Figure 3E) with a concomitant decrease in STxB fluorescence intensity of the limiting membrane (Figure 3E, inset). This situation mirrored the one observed on cells where tubule integrity was specifically affected upon temperature shift only in the presence of normal levels of plasma membrane cholesterol

(G and H) Cell-surface inaccessibility assay was performed as in (D) with MESNA treatment at 4°C on energy-depleted (G) or control cells (H) that were cholesterol extracted with the indicated concentrations of mßCD. Bars = 5 μm.

See also Figures S1 and S2.

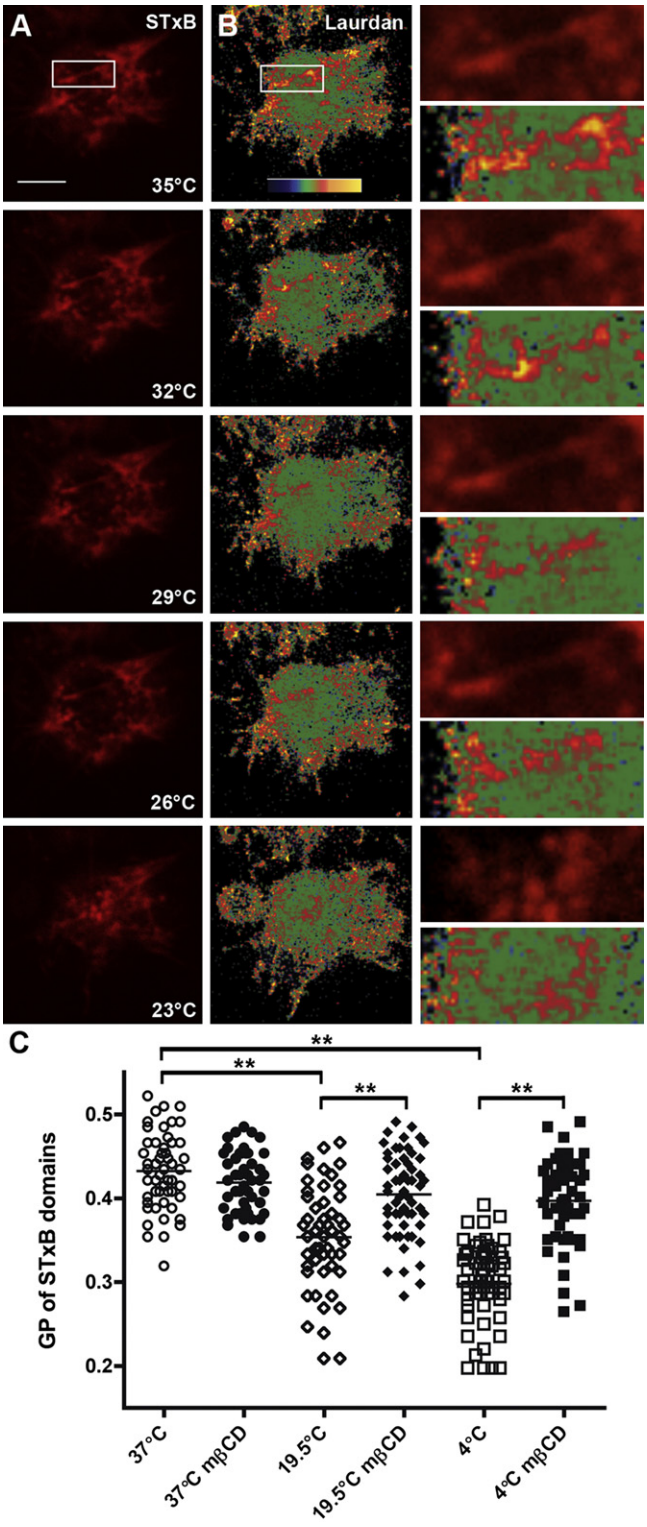

Figure 2. Laurdan Fluorescence Reveals Temperature Shift-Induced Membrane Reorganization on STxB-Induced Tubules

Temperatures were decreased from 37°C to 23°C, and STxB-induced membrane tubules (A) and GP values (B) were imaged in energy-depleted HeLa cells. GP values (pseudocolored; high to low order is yellow to green) change prior to tubule scission. Bar = 10 μm.

(C) Quantitative analysis of the cholesterol-dependent change of GP values with temperature. Means of three independent experiments of ~50 cells are indicated by horizontal lines. **$p < 0.001$ (Tukey's multiple comparison test). See also Figure S3.

(Figure 1C). These reconstitution data established that scission is an intrinsic physical property of the system that can occur in the total absence of cellular pinchase activity.

STxB also induced tubular invaginations on GUVs made with Gb3 from toxin-insensitive erythrocytes (Figure 3F). However, these tubules failed to undergo scission upon temperature shift to 4°C, even in the presence of cholesterol. The most striking difference in the molecular composition of Gb3 preparations from both cells types is the presence of high amounts of α-hydroxylated Gb3 species in HeLa cells (Figure S4). To test whether this lipid species was critical for the scission process, GUVs were reconstituted with purified Gb3 fractions from erythrocytes that contained α-hydroxylated Gb3 species or not. When α-hydroxylated Gb3 was used (Figure 3G), tubules that had formed at 37°C (left image) underwent scission upon shift to room temperature (not shown) or 4°C (right image). In contrast, on GUVs containing non-α-hydroxylated Gb3 (Figure 3H), temperature shift to 4°C did not induce scission, showing that the presence of α-hydroxylated Gb3 species produced a scission-prone membrane environment.

α-hydroxylated glycosphingolipid species have been shown to influence domain size and coverage in lipid bilayers (Windschiegl and Steinem, 2006), and we therefore addressed the importance of domain formation in the scission process in further detail. STxB-induced tubules are too dynamic on GUVs to be imaged in a repetitive manner. To circumvent this technical problem, membrane tubules, or tethers, were mechanically pulled from liposomes, a procedure by which they were immobilized in space and could be followed over time. The liposomes, prepared by the reverse emulsion technique (Pautot et al., 2003) at low temperatures, contained STxB in the lumen so that the appropriate membrane composition resulted in membranes with fully segregated STxB domains prior to tether formation. On liposomes containing HeLa cell Gb3 but no cholesterol, STxB (red) localized into tethers (Figure 4A) and appeared to be enriched (Figure S5A), demonstrating the effective binding to the tether membrane. Under these conditions, tethers were stable for at least as long as 20 min. Tethers were also stable if GUVs were made without STxB, regardless of the presence (Figure S5B) or absence (Figure S5C) of cholesterol. In striking contrast, tethers pulled from liposomes containing HeLa cell Gb3 and cholesterol were stable only for seconds and then rapidly underwent scission before STxB localization could be optically detected (Figure 4B). Tether stability tightly correlated with the presence of STxB domains on the limiting membrane: in cholesterol-containing membranes, domains were clearly present (Figure 4B, arrows) and tethers underwent scission, whereas in membranes without cholesterol, no domain formation was detected and tethers remained stable (Figure 4A).

The correlation between domain formation and scission was further confirmed in experiments using erythrocyte Gb3. In liposomes made with this lipid preparation, no domain formation was observed, and tethers remained stable over extended

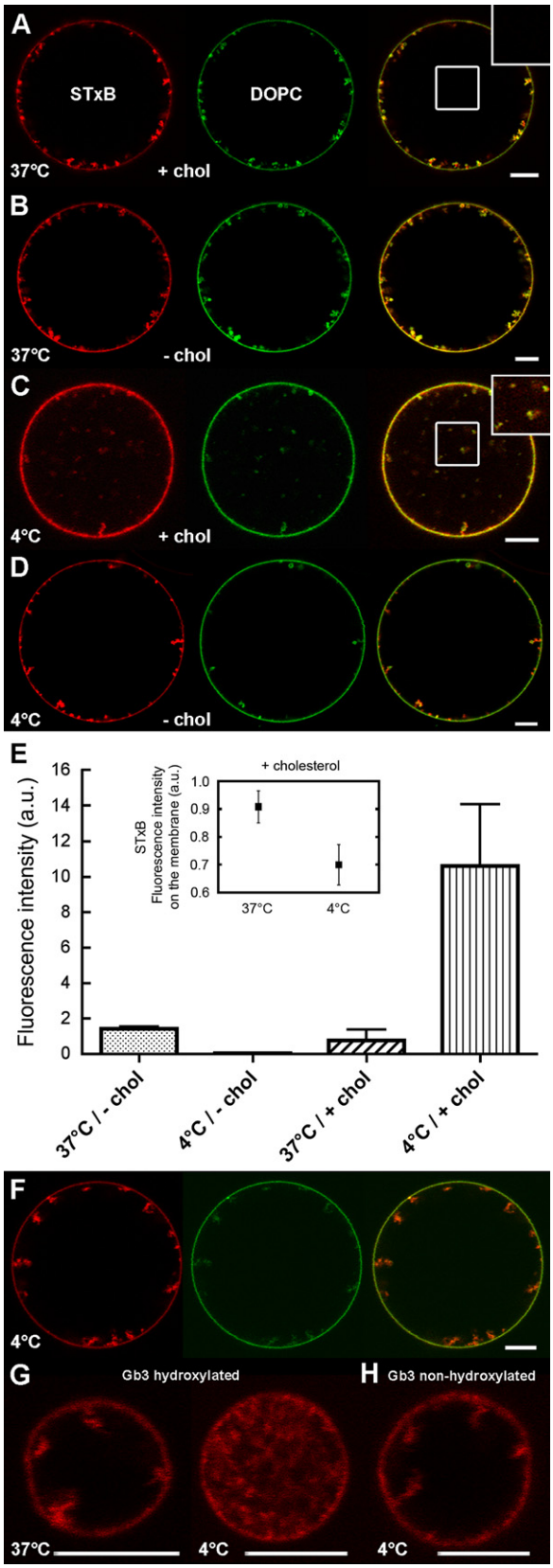

Figure 3. Temperature- and Cholesterol-Dependent Scission of STxB-Induced Membrane Tubules in GUVs

(A–E) GUVs were composed of DOPC (spiked with 1 mol% BodipyFL-C5-HPC, green), HeLa cells Gb3 (5 mol%), containing cholesterol (30 mol%; A and C) or not (B and D). In all conditions, STxB (red) was incubated with GUVs at 37°C and induced tubules. The GUVs were then either further incubated at 37°C (A and B) or shifted to 4°C (C and D). Note that membrane fragments within the GUV lumen were only observed upon temperature shift to 4°C in the presence of membrane cholesterol (C). (E) Quantitative analysis of STxB fluorescence inside GUVs. Means ± standard deviation (SD) of measurements on 35 GUVs. Inset: STxB fluorescence on the limiting cholesterol-containing membrane at the indicated temperatures.

(F) GUVs were composed of DOPC (spiked with 1 mol% BodipyFL-C5-HPC, green), cholesterol (30 mol%), and erythrocyte Gb3 (5 mol%). Tube formation was induced at 37°C. After temperature shift to 4°C, STxB-induced membrane invaginations failed to undergo scission.

(G) On GUVs containing α-hydroxylated Gb3 species (5 mol%, purified bottom spot of erythrocyte Gb3), STxB-induced tubules formed at 37°C (left image) and underwent scission after temperature shift to 4°C (right image).

(H) On GUVs containing non-α-hydroxylated Gb3 species (5 mol%, purified top spot of erythrocyte Gb3), a temperature shift to 4°C did not induce scission.

Bars = 5 μm. See also Figure S4.

periods of time (Figure 4C) that allowed for STxB accumulation (Figure S5D), even in the presence of cholesterol. Taken together, these data demonstrate that scission of STxB-induced membrane invaginations is an intrinsic property of the tubular membrane environment, and it requires specific Gb3 compositions and cholesterol-dependent domain formation.

Actin-Dependent Changes of Membrane Organization in STxB-Induced Tubules

From above it appears that membranes in STxB-induced invaginations are prone to undergo scission by triggered reorganization resulting in domain formation. We hypothesized that actin might be a physiological scission trigger by influencing lipid segregation. Indeed, actin polymerization on membranes increases the temperature at which a phase-separated lipid system becomes homogenous, termed miscibility temperature, and thereby favors phase separation (Liu and Fletcher, 2006). Operationally, the actin polymerization effect on membranes can be equated to temperature shift.

Previous experiments using latrunculin A indicated that actin is required for scission of STxB-induced tubules (Römer et al., 2007). To test the specific involvement of the Arp2/3 complex, the main nucleator of actin polymerization, in the scission process, we depleted the Arp2 protein using siRNAs (see Figure S1). Incubation of STxB with Arp2-depleted cells for 5 min at 37°C led to the appearance of STxB-containing tubular structures (Figure 5A). The actin signal that remained under these conditions did not decorate the tubules.

We next analyzed whether actin was normally associated with STxB-induced tubules. Their scission was inhibited by energy depletion and fixation at 37°C, thereby facilitating microscopic observation. In the vast majority of images, actin could be detected on STxB-containing tubular structures (Figure 5B). The tubule localization of actin was sensitive to cholesterol levels, as shown by the absence of actin signal on STxB-induced

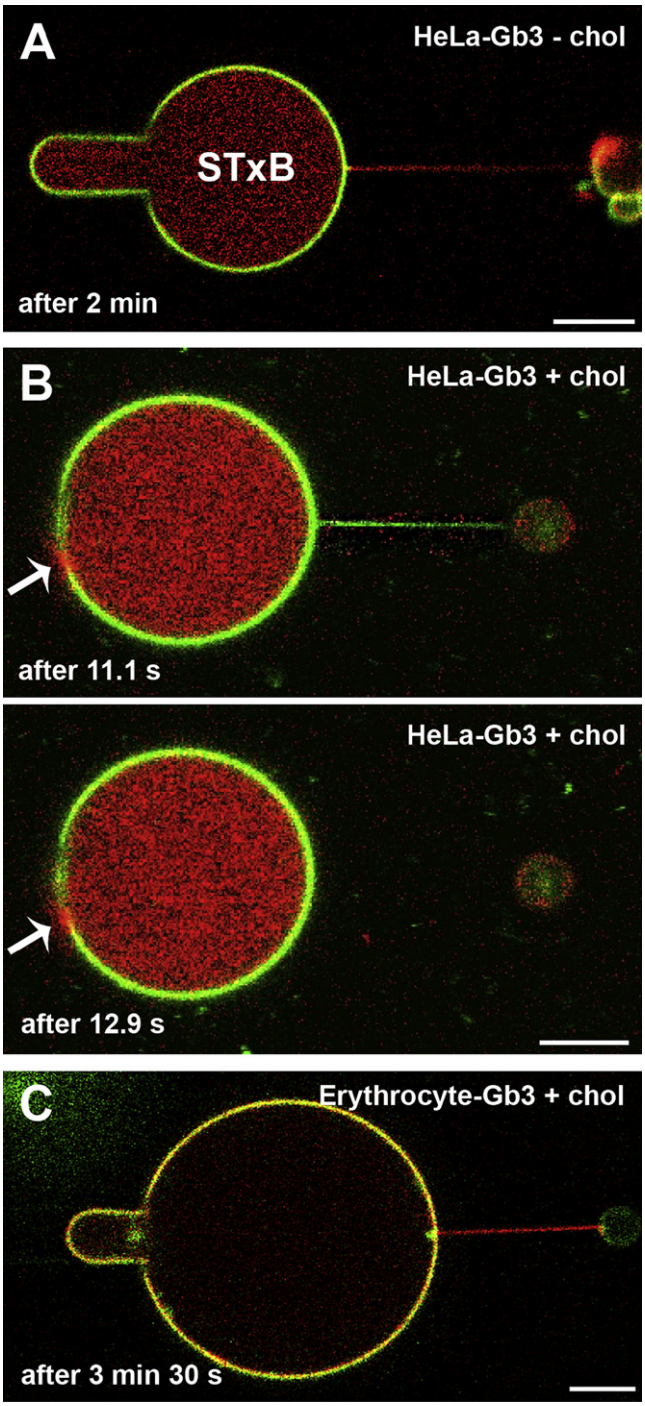

Figure 4. Correlation between Tether Scission and Domain Formation

Bulk membrane (BodipyFL-C5-HPC) is shown in green.

(A) A tether was mechanically pulled from a liposome containing 5 mol% HeLa cell Gb3 in the absence of cholesterol. STxB (red) localized into the tether membrane, which did not break for at least 5 min in 10 out of 10 experiments. The pipette aspiration tongue is visible to the left.

(B) Tether from liposomes with 5 mol% HeLa cell Gb3 and 30 mol% cholesterol. The tether broke before STxB (red) accumulation inside the tube was visible. Note the presence of an STxB domain on the limiting membrane (arrow). The aspiration tongue is not visible in the focal plane of observation. In this setup, 16 out of 21 (76%) tethers broke within 5 min with an average scission time of 19 ± 16 s (SEM).

(C) Tether from liposomes with 5 mol% erythrocyte Gb3 and 30 mol% cholesterol. STxB (red) localized into the tether membrane, which did not break for at least 5 min in 15 independent experiments. The tongue in the aspiration pipette is visible on the left.

Note the absence of STxB domains in (A) and (C). See also Figure S5.

invaginations in cells from which cholesterol was extracted (Figure 5C).

The dynamics of actin polymerization in relation to scission was then analyzed using total internal reflection fluorescence (TIRF) microscopy. STxB-induced tubules that had accumulated under energy depletion conditions were concomitantly imaged for STxB and filamentous actin, using the Lifeact reporter (Riedl et al., 2008). Fluorescence recovery after photobleaching (FRAP) experiments showed that actin was hardly mobile under these conditions (Figure 5D, left column; Figure 5E, blue traces; Movie S1), and remaining recovery may have resulted from passive exchange due to the high dissociation rate of Lifeact (Riedl et al., 2008).

We then exploited the fact that energy depletion is a reversible process (Römer et al., 2007). Shortly after washout of the energy depletion cocktail, actin mobility was strongly increased on STxB-induced tubules (Figure 5D, second column at 1 min after washout; Figure 5E, black traces; Movie S2), and these tubules subsequently underwent scission with a delay after washout as cellular ATP stores were progressively replenished (Figure 5D, 1–3.5 min kinetics and Movie S2). Particularly striking, scission events from the yellow-boxed areas of Figure 5D are shown in Figures 5F and 5G and Movie S2. Clearly, actin polymerized on STxB-induced tubules during the scission process.

We have shown above that temperature shift-triggered scission of STxB-induced tubules was preceded by changes in membrane organization. We used again Laurdan fluorescence to test whether actin also had an effect on membrane organization (Figure 6). The washout of energy-depleting poisons was in this case performed in the absence (Figure 6A) or the presence (Figure 6B) of the actin polymerization inhibitor latrunculin B. In the absence of the inhibitor, STxB (red)-induced tubules underwent scission within minutes (Figure 6A; t = 5.5 min, arrow in inset). Importantly, a change in average membrane order was initiated prior to the scission step (Figure 6A, pseudocolored GP images, same coloring as in Figure 2), such that at 2.5 min the average GP value of the STxB tubule was already strongly reduced while the STxB tubule was still intact with unchanged geometry (see line scans in Figures S6A–S6C).

The quantitative and time-resolved analyses of actin-triggered pre-scission membrane reorganization are presented in Figure 6C for three experiments. In all cases, a small increase in GP values within the first minute of washout was followed by a strong decrease, indicating that membrane reorganization was completed before the tubules underwent scission (arrow in Figure 6C). A time delay between membrane reorganization and scission has been observed previously (Roux et al., 2005) and likely stems from the time it takes for a tubule membrane to constrict at domain boundaries and to drain out the internal liquid.

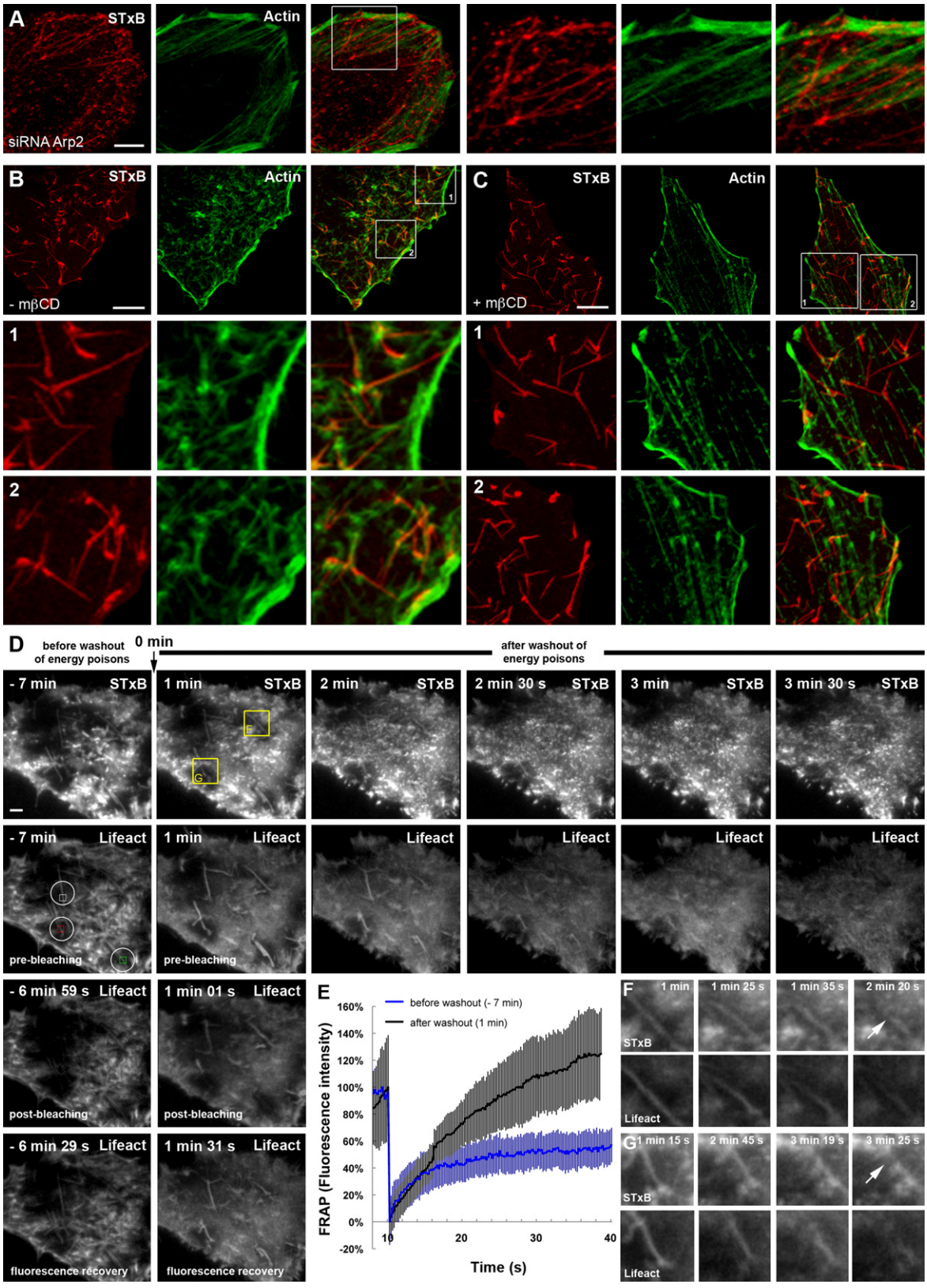
A
STxB
Actin
siRNA Arp2
B
STxB
Actin
- mβCD
C
STxB
Actin
+ mβCD
1
2
D
before washout of energy poisons
0 min
after washout of energy poisons
- 7 min STxB
1 min STxB
2 min STxB
2 min 30 s STxB
3 min STxB
3 min 30 s STxB
- 7 min Lifeact
1 min Lifeact
Lifeact
pre-bleaching
- 6 min 59 s Lifeact
1 min 01 s Lifeact
post-bleaching
- 6 min 29 s Lifeact
1 min 31 s Lifeact
fluorescence recovery
E
before washout (- 7 min)
after washout (1 min)
FRAP (Fluorescence intensity)
160%
140%
120%
100%
80%
60%
40%
20%
0%
-20%
10
20
30
40
Time (s)
F
1 min
1 min 25 s
1 min 35 s
2 min 20 s
STxB
Lifeact
G
1 min 15 s
2 min 45 s
3 min 19 s
3 min 25 s
STxB
Lifeact

In the presence of latrunculin B, STxB (red)-induced tubules failed to undergo scission for more than 10 min after energy poison washout (Figures 6B and 6D). Strikingly, the GP value also did not change (details in Figure 6B; quantification in Figure 6D; line scans in Figure S6), thus demonstrating that actin dynamics influences membrane organization and drives the scission reaction.

Reconstitution of Cholesterol-Dependent Actin-Triggered Tubule Scission without Dynamin

The experiments described above suggest a role for actin in the endocytic processing of STxB-induced membrane invaginations. The temperature and cholesterol dependency of scission and the strict correlation of scission with changes in membrane organization raised the possibility that actin may trigger scission directly and independently of dynamin. We therefore exploited the capacity of STxB to induce membrane invaginations on liposomes (Figure 3) to generate a model membrane system that also includes actin. The actin machinery (actin, the Arp2/3 complex, VVCA-His, ADF/cofilin, and gelsolin) was encapsulated in liposomes by the inverted emulsion technique. All compounds were at least 99% pure, and we could not detect dynamin in the actin mix using immunoblotting (not shown). The nucleation of actin underneath the membrane was driven by the activator fragment VVCA of N-WASP (neuronal Wiskott Aldrich Syndrome Protein), grafted to the membrane by a histidine-nickel interaction. Actin polymerization was triggered by diffusion of salts and ATP into the liposomes through small α-hemolysin-induced membrane pores. Thereby, an actin shell at the inner membrane leaflet could be generated that mimicked the actin cortex of cells (Pontani et al., 2009).

Liposomes were made of egg phosphatidyl choline, Ni-lipids (5 mol%), and Gb3 (5 mol%) in the presence (15 mol%; Figures 7A–7C) or in the absence of cholesterol (Figures 7D–7F). In the presence of cholesterol, STxB induced tubular membrane invaginations on 81% (n = 31) of these liposomes (not shown). The presence of α-hemolysin did not compromise this activity, as 87% (n = 15) of the α-hemolysin-treated liposomes displayed tubular membrane invaginations (Figure 7A, black bar; condition 1). When the nonpolymerized actin mix was included inside the liposomes (absence of α-hemolysin), the percentage of liposomes with tubules (83%, n = 29) did not change significantly (Figure 7A, striped bar; condition 2). In contrast, when cortical actin polymerization was triggered in the presence of cholesterol, a dramatically reduced percentage of liposomes (14%, n = 29) still displayed STxB-induced tubules (Figure 7A, open bar; condition 3), suggesting that scission took place.

Examples of cholesterol-containing liposomes in the different conditions are shown in Figure 7B. In phase contrast images (lower panel), condition 2 (no α-hemolysin, with actin cocktail) appears darker, due to the fact that sucrose could not diffuse out of the liposome. Actin monomers (middle panel) appear diffuse in the nonpolymerized state (condition 2), whereas a cortical actin shell can clearly be seen in condition 3 (with α-hemolysin and actin cocktail). STxB-induced tubules (upper panel) are readily detectable in conditions 1 (with α-hemolysin, no actin cocktail) and 2, but not more in condition 3.

These experiments suggested that actin polymerization triggered the scission of STxB-induced tubular membrane invaginations. Indeed, in about half of the cases of cholesterol-containing liposomes that lacked tubules (condition 3), membrane fragments could be optically resolved in the liposomal lumen (Figure 7C, top inset). In the other half, their presence could only be detected by an increase of the intralumenal STxB fluorescence (Figure 7C, bottom inset and Figure 7B, condition 3), suggesting that the generated membrane fragments were too small to be resolved by light microscopy. This fluorescence increase was further quantified by measuring the fluorescence contrast between the limiting membrane and the liposomal lumen (Figure 7C). The values were similar for conditions 1 and 2 (STxB-induced invaginations remain connected to the limiting membrane, leading to a sharp fluorescence contrast between the limiting membrane and the empty liposomal lumen), whereas the fluorescence contrast strongly decreased in condition 3 due to the appearance of fluorescent membranes within the liposomal lumen. The intralumenal STxB fluorescence was indeed significantly higher in condition 3 (422 ± 76 arbitrary units [a.u.]) than in conditions 1 (222 ± 47 a.u.) and 2 (219 ± 51 a.u.). These findings thereby demonstrate that in the presence of cholesterol, STxB-induced tubules undergo scission in liposomes with cortical actin.

The specificity of this process was demonstrated by omission of the VVCA fragment and Arp2/3 complex from the actin cocktail. No cortical actin shell was observed under these conditions (Figure S7A) and liposomes still displayed tubules (Figure S7B, condition 2′) as observed in the absence of actin polymerization when no ATP was present (condition 2). The fluorescence contrast between limiting membrane and the liposomal lumen

Figure 5. Actin Dynamics on STxB-Induced Tubular Membrane Invaginations

(A) The occurrence of STxB-induced tubules (5 min incubation) is strongly increased on HeLa cells that were depleted for Arp2, suggesting that the Arp2/3 complex is required for scission.

(B and C) HeLa cells were energy depleted and mock extracted (B) or cholesterol extracted (C). STxB (red) induced tubules in both conditions, but actin was only found on tubules in cells that were not cholesterol depleted (B).

(D) Life cell imaging and FRAP analysis of actin dynamics on STxB-induced membrane tubules before and during membrane scission. HeLa cells were transfected with mcherry-Lifeact plasmid, energy-depleted, and incubated with STxB-Alexa488. Membrane scission following washout (0 min) of the energy poisons was followed over time. Regions indicated by white open circles were photobleached for 10 ms at −7 min (left column) and at +1 min (2nd column) with respect to washout with a 561 nm laser, and fluorescence recovery of mcherry-Lifeact was measured. Regions indicated by small colored squares were chosen for FRAP analysis.

(E) FRAP data are plotted as average fluorescence intensity (± SD) of mcherry-Lifeact. The blue curve represents actin recovery on STxB tubules in energy-depleted cells (FRAP at −7 min). The upper black curve represents actin recovery on STxB tubules in the same cells after washout (FRAP at +1 min).

(F and G) Two scission events (yellow open squares in D) are shown at higher magnification. Arrows highlight scission events.

Bars = 5 μm. See also Movies S1 and S2.

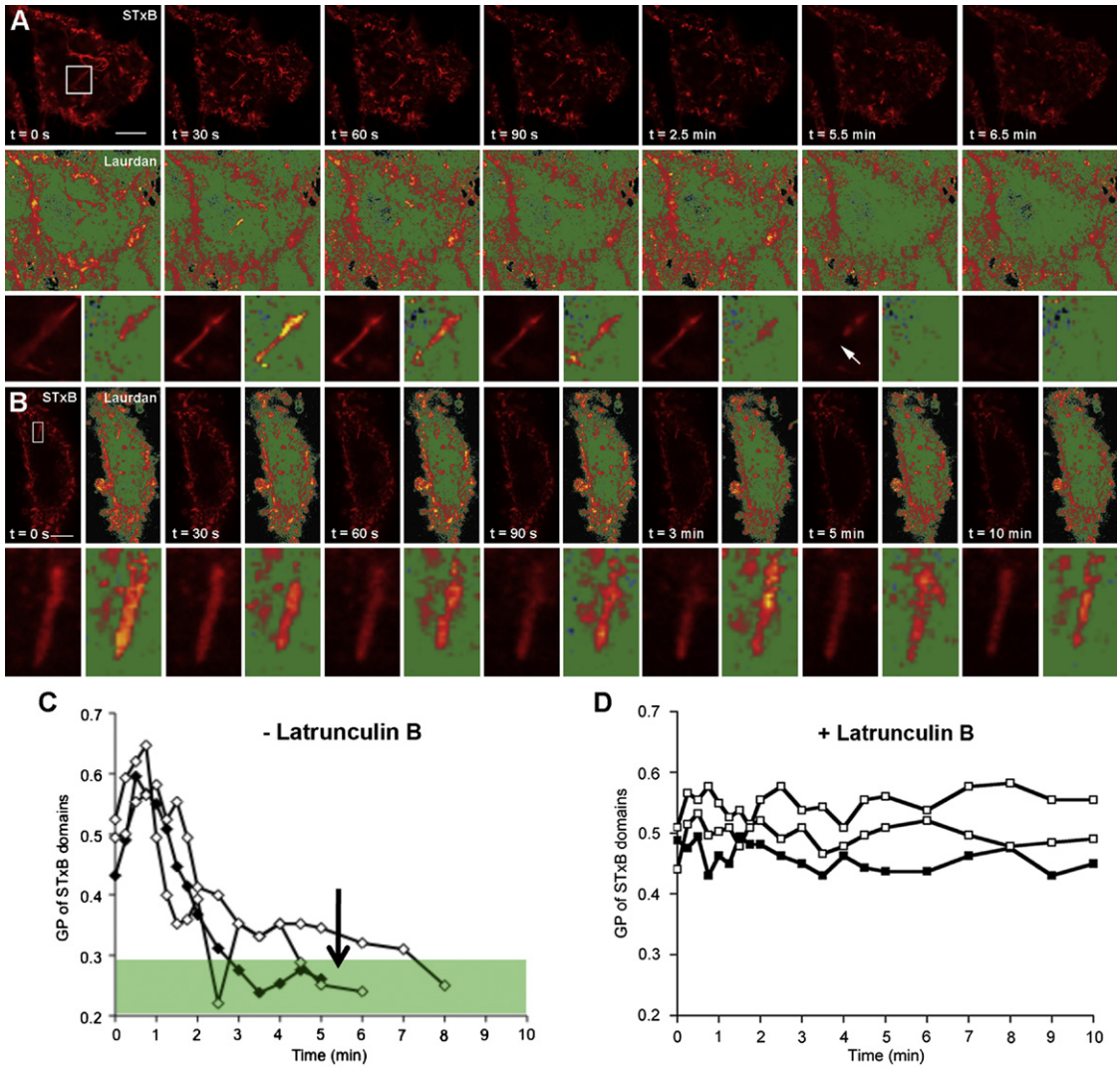

Figure 6. Actin Triggers Membrane Reorganization and Drives Membrane Scission

STxB tubules (red) and membrane order (pseudocolored GP images) were followed during a washout period with PBS^{2+} in the absence (A) or presence (B) of 10 μM latrunculin B. STxB tubules were formed in energy-depleted HeLa cells prior to imaging. Bars = 10 μm. (C) and (D) show GP values of individual STxB tubules, with filled symbols showing tubules of (A) and (B), respectively. The green shaded region in (C) denotes the GP values of the membranes surrounding the STxB tubules, and the arrow indicates the time of scission of the tubule shown in (A) (filled symbols).
See also Figure S6.

did not change either (Figure S7C) demonstrating that in the absence of VVCA fragment and Arp2/3, no scission occurred.

In the absence of cholesterol, STxB induced tubules in 71% (n = 14) of liposomes, a value that is in the same range as observed on cholesterol-containing liposomes (see above) and that was not affected by α-hemolysin (Figure 7D, condition 1; 71%, n = 15) or nonpolymerized actin (Figure 7D, condition 2; 67%, n = 31). Strikingly, in marked contrast to cholesterol-containing liposomes, this percentage was not affected by actin polymerization (Figure 7D, condition 3; 70%, n = 23). STxB-induced tubules were indeed clearly visible in liposomes in which a cortical actin shell had formed (Figure 7E, condition 3). Correspondingly, the contrast of the STxB fluorescence signal remained stable in all conditions (Figure 7F). These findings faithfully reproduce the observations made with cells and demonstrate that actin can trigger the scission of STxB-induced tubules in the absence of dynamin and in a manner that critically depends on membrane cholesterol levels.

DISCUSSION

Membrane scission is one of the key events in vesicular transport. It requires localized constriction of opposing segments of the same membrane, thereby causing the physical separation of the bud from the donor membrane. We have found that a temperature shift leads to a change in membrane organization at the site of STxB-induced tubular membrane invaginations. This change precedes scission, even in conditions under which

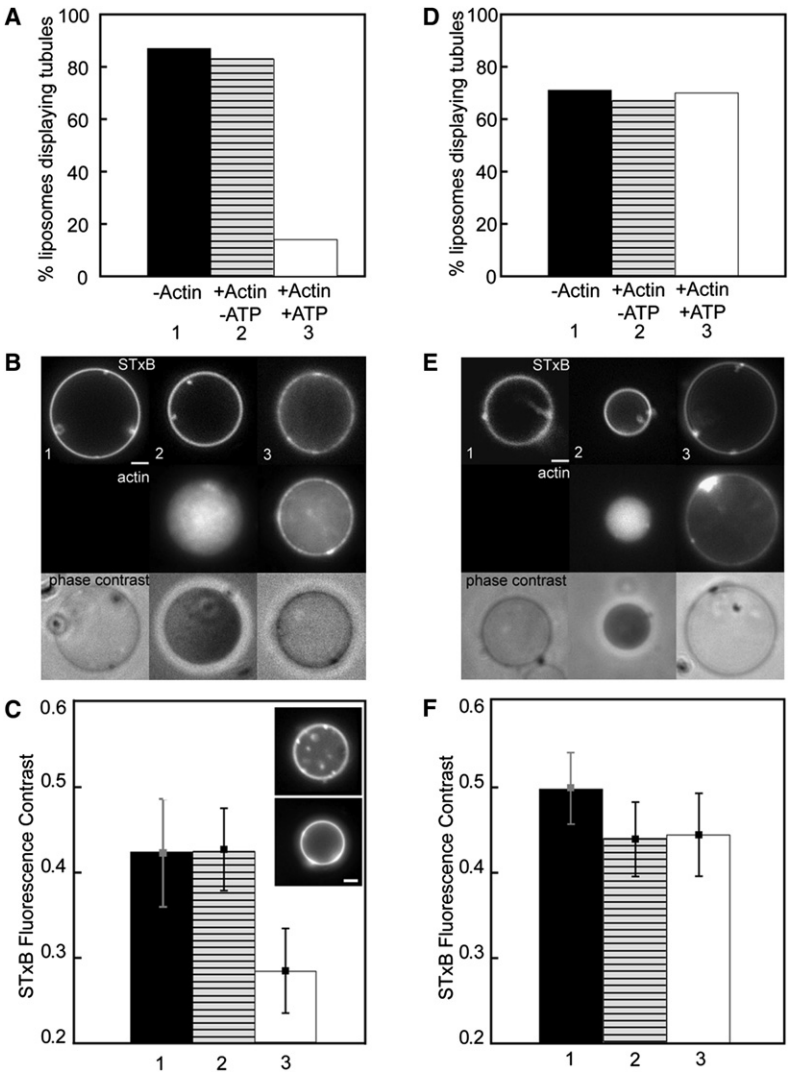

Figure 7. Reconstitution of Cholesterol-Dependent, Actin-Triggered Tubule Scission in Liposomes

Liposomes were composed of egg phosphatidyl choline, erythrocyte Gb3 (5 mol%), and DOGS-NTA-Ni (5 mol%), containing (A–C) or not (D–F) 15 mol% of cholesterol. In all cases, STxB induced membrane invaginations. Three conditions were studied: (1) With α-hemolysin and without actin; (2) with nonpolymerized actin inside the liposomes (no α-hemolysin); (3) the full system with polymerized actin, i.e., with both α-hemolysin and actin cocktail.

(A) With cholesterol-containing membranes, the percentage of liposomes displaying tubules strongly decreases upon cortical actin polymerization (condition 3).

(B) Images of the liposomes in epifluorescence (STxB and actin) and phase contrast mode. In condition 3, actin fluorescence localizes at the membrane, and STxB fluorescence is increased in the liposomal lumen.

(C) Quantification of lumenal STxB fluorescence contrast (see Experimental Procedures). Means ± SD of measurements on 10–30 liposomes. Note the drop of contrast in condition 3. Inset: Among the liposomes with no tubules close to the membrane (80%), the presence of STxB inside the liposome is characterized either by resolved membrane elements (top) or a diffuse fluorescence signal (bottom).

(D) In liposomes without cholesterol, the percentage of liposomes displaying tubules is similar in all conditions.

(E) Refer to (B) for details, except that in the absence of cholesterol, cortical actin polymerization does not induce tubule scission.

(F) The STxB fluorescence contrast between lumen and limiting membrane are similar in all conditions.

Bars = 2 μm. See also Figure S7.

active cellular machinery is inhibited, suggesting that within the invaginations, membranes are prone to undergo spontaneous breakage. Our data on cells and model membranes suggest that localized actin polymerization is a physiological trigger for scission.

A Physical Mechanism of Scission

Domain formation generates strain at domain boundary regions, termed line tension. The energy of a membrane system with domains can therefore be minimized by decreasing the total length of such domain boundaries. Theoretical considerations show that when domain formation occurs in membrane tubules, the minimization of the line energy of the system (i.e., the shortening of the circumferential area at domain boundaries) leads to the spontaneous constriction of the tubule and might result in scission (Allain et al., 2004). Additional mechanical force provided by actin may further favor the process (Liu et al., 2006). Line tension-driven scission has been documented in model membrane systems with membrane tethers pulled from GUVs (Roux et al., 2005), but not yet on cells. The experimental observations of our study strongly suggest that scission of STxB-induced cellular endocytic tubules is governed by similar principles.

A corollary of this model is that membranes in STxB-induced tubular invaginations have to be close to a lipid demixing point at physiological temperature, such that an appropriate trigger (in this study: temperature shift or actin polymerization) induces domain formation, line tension, and scission. Recent studies provide compelling evidence for biological membrane preparations of different origins that are indeed homogenous at 37°C but undergo liquid-liquid phase separation upon lowering temperature for as little as a few degrees (Baumgart et al., 2007; Heimburg and Jackson, 2005; Lingwood et al., 2008; Polozov et al., 2008). This effect was particularly striking in a lipid preparation from influenza virus (Polozov et al., 2008) that has been described to be enriched in so-called raft lipids, i.e., cholesterol and sphingolipids (Scheiffele et al., 1999).

Several independent lines of evidence from this and previous studies suggest that membranes in STxB-induced tubules are close to such a demixing point: STxB, like influenza virus proteins, is found in detergent-resistant membrane extracts (Falguières et al., 2001) and in highly ordered membrane domains (Römer et al., 2007), suggesting that STxB resides

in a raft-like membrane environment. Furthermore, we found here that triggering scission of STxB-induced tubules by temperature shift is sensitive to cholesterol levels in cell and model membranes. This cholesterol dependency can be explained by the established effect of sterols (Bacia et al., 2005) and temperature (Honerkamp-Smith et al., 2008; McConnell and Vrljic, 2003) on phase separation and line tension. Indeed, we demonstrate that the cholesterol-dependent formation of STxB domains directly correlates with tether scission in a model membrane system. Finally, we measured that STxB membranes in cells underwent reorganization prior to tubule scission.

Although the exact organization of the STxB-Gb3 domains has not yet been determined, we observed that GP values drop prior to scission induced by the temperature shift or actin polymerization. To explain this finding, we propose two nonexclusive possibilities that are both based on the assumption that STxB-induced tubular membranes reorganize into domains, some of which may be too small to be detected optically. Our GP measurements represent the average GP values to which all the domains are contributing. The first possibility is that the segregation of ordered membranes in STxB-induced tubules into highly ordered and less ordered domains may decrease the average GP value. This is because the amplitude of GP differences varies with different types of phase transitions, in which a shift toward less ordered membranes results in a greater decrease in GP than a shift to more ordered membranes causes an increase in GP (Dietrich et al., 2001). Second, other members of the Laurdan dye family partition preferentially into the fluid phase (see for example Prodan; Bagatolli and Gratton, 2000). Although it has been described that Laurdan itself does not discriminate between liquid-ordered or liquid-disordered phases (Bagatolli and Gratton, 2000; Kaiser et al., 2009), it is possible that the dye is excluded from highly ordered lipid nano-clusters. Nano-clusters or other domains, even if they are too small to be resolved optically, generate boundary forces, thereby driving the scission process.

Physiological Scission Triggers

From the argument above arises the need to identify inducers that trigger membrane reorganization and domain formation at physiological temperature, thereby leading to scission. Our work strongly suggests that actin polymerization is one of these scission triggers. Indeed, in a dynamin-free model membrane system that is entirely reconstituted from synthetic or highly purified compounds, STxB-induced tubules are stable in the presence of monomeric actin, while polymerization of cortical actin readily triggers scission in a process that is sensitive to membrane cholesterol.

Actin may trigger scission via several nonexclusive mechanisms. The cholesterol dependency of actin-triggered scission in our model membrane system and the correlation between stable membrane order and absence of scission when actin polymerization is inhibited in cells point to an involvement of lipid repartition effects and line tension squeezing as one of the possible mechanisms. As it has been mentioned in the Results section, the polymerization of actin on model membranes increases the miscibility temperature (Liu and Fletcher, 2006), which equates a shift to lower temperatures. This effect may arise from actin filaments binding to lipids such as phosphatidylinositol-4,5-bisphosphate, counterbalancing entropy loss that arises from lipid segregation and thereby favoring domain formation.

A complementary mechanism by which actin polymerization could drive scission is through mechanical force on the membrane. Indeed, line tension may not be sufficient to get opposing membranes into a fusion-compatible distance (Liu et al., 2006), and actin polymerization may provide additional mechanical stress that could squeeze or pull the membrane. In a previous study on another model membrane system, we have indeed demonstrated such fission-promoting forces caused by actin polymerization (Heuvingh et al., 2007).

The dynamin-independent line tension-driven scission mechanism described here may in some cases operate in synergy with dynamin, as for Shiga toxin uptake. A possibility is that dynamin, by virtue of its interaction with membrane lipids (i.e., phosphatidylinositol-4,5-bisphosphate), might contribute to domain formation and lipid segregation, which could favor membrane fission (discussed in Liu et al., 2009). In other circumstances, the line tension-driven mechanism may operate on its own right. One example is SV40. Similar to Shiga toxin, this virus induces endocytic membrane invaginations (Ewers et al., 2010), which are then processed independently of dynamin (Damm et al., 2005). Some endogenous trafficking processes also have the dynamic formation of raft-like nanodomains and the appearance of tubular endocytosis intermediates in common with Shiga toxin. A well-studied example is the dynamin-independent GEEC pathway for the uptake of GPI-anchored proteins (Mayor and Pagano, 2007). In yeast, dynamin is not expressed and scission of tubular endocytic structures occurs following the recruitment of the actin module (Kaksonen et al., 2005). Sterols and sphingolipids play important roles in yeast endocytosis (Souza and Pichler, 2007), and it remains to be determined to what extent they contribute with phosphatidylinositol-4,5-bisphosphate to the scission process.

In conclusion, our study provides a conceptual framework for a dynamin-independent scission mechanism in endocytosis that implicates as the driving forces actin polymerization combined with the intrinsic physical property of specific membranes to undergo rearrangements at scales larger than molecular that result in domain formation and line tension-driven tubule constriction.

EXPERIMENTAL PROCEDURES

List of Materials is in the Extended Experimental Procedures.

Cell Culture

HeLa cells were grown at 5% CO_2 in DMEM (GIBCO BRL) medium containing 4.5 g/l glucose supplemented with 10% FCS, 0.01% penicillin-streptomycin, 4 mM glutamine, and 5 mM pyruvate.

RNA Interference

Small-interfering RNAs (siRNAs) to deplete hArp2 were obtained from Santa Cruz. HeLa cells were transfected in six-well dishes with Oligofectamine (Invitrogen) according the manufacturer's instructions. Experiments were performed after 3 days of transfection.

Depletion of Cellular Energy

Cellular energy was depleted by incubating HeLa cells in PBS^{2+} supplemented with 10 mM 2-deoxy-D-glucose and 10 mM NaN3 for 30 min at 37°C (Römer et al., 2007). Control cells were incubated with PBS^{2+} supplemented with 5 mM glucose.

Biochemistry and Internalization Assay

STxB and Tf were conjugated to biotin via a cleavable (MESNA-sensitive) disulfide bond, using the biotinylating agent Sulfo-NHS-SS-biotin (Pierce). Endocytosis was measured as the percentage of internalized STxB (+MESNA sample) divided by total cell-associated STxB (-MESNA sample), as previously described (Amessou et al., 2006; Mallard and Johannes, 2003). Cholesterol was extracted from cells with methyl-β-cyclodextrin (Falguières et al., 2001).

Immunofluorescence and Confocal Microscopy

Immunofluorescence studies were carried out as previously described (Mallard et al., 1998). For lifetime imaging, HeLa cells were grown to subconfluence on FluoroDish chambers with integrated glass coverslips (World Precision Instruments, Inc).

Laurdan Experiments

HeLa cells were energy depleted, labeled with Laurdan, cholesterol depleted, and incubated with Cy3-STxB as previously described (Römer et al., 2007). Laurdan intensity images were recorded with a 2-photon DM IRE2 Microscope (Leica, Australia) on a temperature-controlled stage, converted into general-polarization (GP) images (ImageJ), and pseudocolored (Adobe Photoshop) (Gaus et al., 2003). Membrane organization of STxB-enriched membranes was carried out by pixel-per-pixel comparisons. Parameters describing global membrane structure were obtained by deconvoluting GP histograms.

GUV Formation and Analysis

Giant unilamellar vesicles (GUVs) of various lipid compositions containing the fluorescent lipid BodipyFL-C5-HPC (1 mol%) were grown using the electroformation technique, essentially as previously described (Mathivet et al., 1996). GUVs were examined under an inverted confocal fluorescence microscope (LSM 510, Carl Zeiss) equipped with a Zeiss ×63 PL APO HCX, 1.4 NA oil immersion objective.

Characterization of STxB Fluorescence on Liposomes

The maximum intensity value along a radius starting from the center of the liposome was measured 360 times by rotating the radius, and the mean maximal intensity ($\overline{M}$) at the membrane was calculated (Römer et al., 2007). The background intensity (m) inside the liposome was measured as the average fluorescence intensity of a centered disk of half the diameter of the liposome. For each experimental condition, 10 to 30 liposomes were analyzed, and results were gathered in a histogram. The STxB contrast in a liposome was defined as $C = \overline{M} - m/\overline{M} + m$ where $\overline{M}$ and m were measured on corresponding images.

Preparation of Actin-Containing Liposomes

Lipid bilayers were made of egg L-α-phosphatidyl choline (75 mol%), cholesterol (15 mol%), porcine erythrocyte Gb3 (5 mol%), and 1,2-Dioleoyl-sn-Glycero-3-([N(5-Amino-1-carboxypentyl)iminodiacetic acid]succinyl)(nickel salt) (DOGS-NTA-Ni, 5 mol%) to bind to the VVCA histidine tag. When cholesterol was omitted, L-α-phosphatidyl choline was used at 90 mol%. Pores (α-hemolysin) were incorporated to allow salt and ATP to flow into the liposome by adding 0.6 μl of 1 mg/ml α-hemolysin directly into the sample before sealing the slide and coverslip chamber for observation. α-hemolysin was in large excess, which allowed instantaneous exchange. A tubule was considered as present as soon as its length exceeded twice the membrane fluorescence thickness.

Tether Pulling

Cy3-STxB (40 μg/ml) was encapsulated in liposomes by reverse emulsion technique, as described above. The buffer solution contained 100 mM NaCl, 20 mM HEPES, 100 mg/ml dextran, and sucrose to match the osmolarity of the outside buffer made of 100 mM NaCl, 20 mM HEPES, 0.5 mg/ml casein, and glucose. The membranes were made of 64 mol% egg phosphatidylcholine (EPC), 30 mol% cholesterol, 1 mol% BodipyFL-C5-HPC, 5 mol% Gb3 from erythrocytes or HeLa cells, and 0.03% of DSPE-PEG2000-biotin. When cholesterol was omitted, the liposomes consisted of 94 mol% EPC. Tether pulling experiments were performed using an original setup described elsewhere (Sorre et al., 2009). Briefly, membrane nanotubes were pulled out of liposomes by a bead (3.2 μm diameter streptavidin-coated polystyrene bead) trapped in an optical tweezer and attached to the membrane through a biotin-streptavidin bond. Membrane tension in the liposome was controlled through micropipette aspiration, the force at which the tether is pulled was measured, and fluorescence was quantified. To prevent adhesion of the vesicles to the glass surface, the open micromanipulation chamber and the micropipette were incubated with β-casein. Tethers were pulled from the liposome to lengths of 10 to 15 μm; this length was then kept constant during the entire experiment. Membrane tension, set via controlled micropipette aspiration, ranged from 5.10^{-6} Nm^{-1} (tube radius ~50 nm) to 2.10^{-4} Nm^{-1} (tube radius ~10 nm). Scission events were scored within a 5 min time window. Experiments were performed at 21 ± 1°C.

SUPPLEMENTAL INFORMATION

Supplemental Information includes Extended Experimental Procedures, seven figures, and two movies and can be found with this article online at doi:10.1016/j.cell.2010.01.010.

ACKNOWLEDGMENTS

We thank Satyajit Mayor, Madan Rao, Pierre Sens, Luis Bagatolli, and Emmanuel Derivery for helpful discussions and Dylan Owen for help in Laurdan experiments. The authors acknowledge the help of the PICT-IBiSA imaging staff and the use of the advanced microscopy equipment of the Nikon Imaging Centre at Institut Curie-CNRS. Our laboratories were supported by Association de Recherche Contre le Cancer (n°3143), Curie Institute (PIC Vectorisation), Agence Nationale pour la Recherche (Physicochimie du Vivant), European Commission (SoftComp, NoE/NMP3-CT-2004-502235), Human Frontier Science Program Organization (RGP26/2007 and RPG58/2005), and ANR program blanc (ProLipScis). W.R. (CNRS), L.B., B.S. (Direction Générale pour l'Armement and Fondation pour la Recherche Médicale), and L.L.P. (French Ministry of Science and Technology) were supported by fellowships from the indicated organizations.

Received: February 19, 2009
Revised: July 29, 2009
Accepted: December 31, 2009
Published: February 18, 2010

REFERENCES

Allain, J.M., Storm, C., Roux, A., Ben Amar, M., and Joanny, J.F. (2004). Fission of a multiphase membrane tube. Phys. Rev. Lett. *93*, 158104.

Amessou, M., Popoff, V., Yelamos, B., Saint-Pol, A., and Johannes, L. (2006). Measuring retrograde transport to the trans-Golgi network, Chapter 15: Unit 15.10. In Current Protocols in Cell Biology, J.S. Bonifacino, M. Dasso, J.B. Harford, J. Lippincott-Schwartz, and K.M. Yamada, eds. (New York: John Wiley & Sons, Inc.)

Bacia, K., Schwille, P., and Kurzchalia, T. (2005). Sterol structure determines the separation of phases and the curvature of the liquid-ordered phase in model membranes. Proc. Natl. Acad. Sci. USA *102*, 3272–3277.

Bagatolli, L.A., and Gratton, E. (2000). Two photon fluorescence microscopy of coexisting lipid domains in giant unilamellar vesicles of binary phospholipid mixtures. Biophys. J. *78*, 290–305.

Baumgart, T., Hammond, A.T., Sengupta, P., Hess, S.T., Holowka, D.A., Baird, B.A., and Webb, W.W. (2007). Large-scale fluid/fluid phase separation of proteins and lipids in giant plasma membrane vesicles. Proc. Natl. Acad. Sci. USA *104*, 3165–3170.

Bonifacino, J.S., and Glick, B.S. (2004). The mechanisms of vesicle budding and fusion. Cell *116*, 153–166.

Bonifacino, J.S., and Rojas, R. (2006). Retrograde transport from endosomes to the trans-Golgi network. Nat. Rev. Mol. Cell Biol. *7*, 568–579.

Damm, E.M., Pelkmans, L., Kartenbeck, J., Mezzacasa, A., Kurzchalia, T., and Helenius, A. (2005). Clathrin- and caveolin-1-independent endocytosis: entry of simian virus 40 into cells devoid of caveolae. J. Cell Biol. *168*, 477–488.

Dietrich, C., Bagatolli, L.A., Volovyk, Z.N., Thompson, N.L., Levi, M., Jacobson, K., and Gratton, E. (2001). Lipid rafts reconstituted in model membranes. Biophys. J. *80*, 1417–1428.

Ewers, H., Römer, W., Smith, A.E., Bacia, K., Dmitrieff, S., Chai, W., Mancini, R., Kartenbeck, J., Chambon, V., Berland, L., et al. (2010). SV40 binding to its receptor, GM1, induces membrane invagination, tubulation, and infection. Nat. Cell Biol. *12*, 11–18.

Falguières, T., Mallard, F., Baron, C.L., Hanau, D., Lingwood, C., Goud, B., Salamero, J., and Johannes, L. (2001). Targeting of Shiga toxin B-subunit to retrograde transport route in association with detergent resistant membranes. Mol. Biol. Cell *12*, 2453–2468.

Gaus, K., Gratton, E., Kable, E.P., Jones, A.S., Gelissen, I., Kritharides, L., and Jessup, W. (2003). Visualizing lipid structure and raft domains in living cells with two-photon microscopy. Proc. Natl. Acad. Sci. USA *100*, 15554–15559.

Goswami, D., Gowrishankar, K., Bilgrami, S., Ghosh, S., Raghupathy, R., Chadda, R., Vishwakarma, R., Rao, M., and Mayor, S. (2008). Nanoclusters of GPI-anchored proteins are formed by cortical actin-driven activity. Cell *135*, 1085–1097.

Guha, A., Sriram, V., Krishnan, K.S., and Mayor, S. (2003). Shibire mutations reveal distinct dynamin-independent and -dependent endocytic pathways in primary cultures of Drosophila hemocytes. J. Cell Sci. *116*, 3373–3386.

Heimburg, T., and Jackson, A.D. (2005). On soliton propagation in biomembranes and nerves. Proc. Natl. Acad. Sci. USA *102*, 9790–9795.

Heuvingh, J., Franco, M., Chavrier, P., and Sykes, C. (2007). ARF1-mediated actin polymerization produces movement of artificial vesicles. Proc. Natl. Acad. Sci. USA *104*, 16928–16933.

Honerkamp-Smith, A.R., Cicuta, P., Collins, M.D., Veatch, S.L., den Nijs, M., Schick, M., and Keller, S.L. (2008). Line tensions, correlation lengths, and critical exponents in lipid membranes near critical points. Biophys. J. *95*, 236–246.

Johannes, L., and Popoff, V. (2008). Tracing the retrograde route in protein trafficking. Cell *135*, 1175–1187.

Kaiser, H.J., Lingwood, D., Levental, I., Sampaio, J.L., Kalvodova, L., Rajendran, L., and Simons, K. (2009). Order of lipid phases in model and plasma membranes. Proc. Natl. Acad. Sci. USA *106*, 16645–16650.

Kaksonen, M., Toret, C.P., and Drubin, D.G. (2005). A modular design for the clathrin- and actin-mediated endocytosis machinery. Cell *123*, 305–320.

Kirkham, M., and Parton, R.G. (2005). Clathrin-independent endocytosis: new insights into caveolae and non-caveolar lipid raft carriers. Biochim. Biophys. Acta *1745*, 273–286.

Lauvrak, S.U., Torgersen, M.L., and Sandvig, K. (2004). Efficient endosome-to-Golgi transport of Shiga toxin is dependent on dynamin and clathrin. J. Cell Sci. *117*, 2321–2331.

Lingwood, D., Ries, J., Schwille, P., and Simons, K. (2008). Plasma membranes are poised for activation of raft phase coalescence at physiological temperature. Proc. Natl. Acad. Sci. USA *105*, 10005–10010.

Liu, A.P., and Fletcher, D.A. (2006). Actin polymerization serves as a membrane domain switch in model lipid bilayers. Biophys. J. *91*, 4064–4070.

Liu, J., Kaksonen, M., Drubin, D.G., and Oster, G. (2006). Endocytic vesicle scission by lipid phase boundary forces. Proc. Natl. Acad. Sci. USA *103*, 10277–10282.

Liu, J., Sun, Y., Drubin, D.G., and Oster, G.F. (2009). The mechanochemistry of endocytosis. PLoS Biol. *7*, e1000204.

Macia, E., Ehrlich, M., Massol, R., Boucrot, E., Brunner, C., and Kirchhausen, T. (2006). Dynasore, a cell-permeable inhibitor of dynamin. Dev. Cell *10*, 839–850.

Mallard, F., and Johannes, L. (2003). Shiga toxin B-subunit as a tool to study retrograde transport, Chapter 17. In Methods in Molecular Medicine: Shiga Toxin Methods and Protocols, Volume 73, D. Philpott and F. Ebel, eds. (Totowa, NJ: Humana Press), pp. 209–220.

Mallard, F., Tenza, D., Antony, C., Salamero, J., Goud, B., and Johannes, L. (1998). Direct pathway from early/recycling endosomes to the Golgi apparatus revealed through the study of Shiga toxin B-fragment transport. J. Cell Biol. *143*, 973–990.

Mathivet, L., Cribier, S., and Devaux, P.F. (1996). Shape change and physical properties of giant phospholipid vesicles prepared in the presence of an AC electric field. Biophys. J. *70*, 1112–1121.

Mayor, S., and Pagano, R.E. (2007). Pathways of clathrin-independent endocytosis. Nat. Rev. Mol. Cell Biol. *8*, 603–612.

McConnell, H.M., and Vrljic, M. (2003). Liquid-liquid immiscibility in membranes. Annu. Rev. Biophys. Biomol. Struct. *32*, 469–492.

Mettlen, M., Pucadyil, T., Ramachandran, R., and Schmid, S.L. (2009). Dissecting dynamin's role in clathrin-mediated endocytosis. Biochem. Soc. Trans. *37*, 1022–1026.

Pautot, S., Frisken, B.J., and Weitz, D.A. (2003). Engineering asymmetric vesicles. Proc. Natl. Acad. Sci. USA *100*, 10718–10721.

Polozov, I.V., Bezrukov, L., Gawrisch, K., and Zimmerberg, J. (2008). Progressive ordering with decreasing temperature of the phospholipids of influenza virus. Nat. Chem. Biol. *4*, 248–255.

Pontani, L.L., van der Gucht, J., Salbreux, G., Heuvingh, J., Joanny, J.F., and Sykes, C. (2009). Reconstitution of an actin cortex inside a liposome. Biophys. J. *96*, 192–198.

Praefcke, G.J., and McMahon, H.T. (2004). The dynamin superfamily: universal membrane tubulation and fission molecules? Nat. Rev. Mol. Cell Biol. *5*, 133–147.

Riedl, J., Crevenna, A.H., Kessenbrock, K., Yu, J.H., Neukirchen, D., Bista, M., Bradke, F., Jenne, D., Holak, T.A., Werb, Z., et al. (2008). Lifeact: a versatile marker to visualize F-actin. Nat. Methods *5*, 605–607.

Römer, W., Berland, L., Chambon, V., Gaus, K., Windschiegl, B., Tenza, D., Aly, M.R., Fraisier, V., Florent, J.-C., Perrais, D., et al. (2007). Shiga toxin induces tubular membrane invaginations for its uptake into cells. Nature *450*, 670–675.

Roux, A., Cuvelier, D., Nassoy, P., Prost, J., Bassereau, P., and Goud, B. (2005). Role of curvature and phase transition in lipid sorting and fission of membrane tubules. EMBO J. *24*, 1537–1545.

Saint-Pol, A., Yélamos, B., Amessou, M., Mills, I., Dugast, M., Tenza, D., Schu, P., Antony, C., McMahon, H.T., Lamaze, C., et al. (2004). Clathrin adaptor epsinR is required for retrograde sorting on early endosomal membranes. Dev. Cell *6*, 525–538.

Sandvig, K., Garred, O., Prydz, K., Kozlov, J.V., Hansen, S.H., and van Deurs, B. (1992). Retrograde transport of endocytosed Shiga toxin to the endoplasmic reticulum. Nature *358*, 510–512.

Scheiffele, P., Rietveld, A., Wilk, T., and Simons, K. (1999). Influenza viruses select ordered lipid domains during budding from the plasma membrane. J. Biol. Chem. *274*, 2038–2044.

Sens, P., Johannes, L., and Bassereau, P. (2008). Biophysical approaches to protein-induced membrane deformations in trafficking. Curr. Opin. Cell Biol. *20*, 476–482.

Sharma, P., Varma, R., Sarasij, R.C., Ira, Gousset, K., Krishnamoorthy, G., Rao, M., and Mayor, S. (2004). Nanoscale organization of multiple GPI-anchored proteins in living cell membranes. Cell *116*, 577–589.

Simons, K., and Vaz, W.L. (2004). Model systems, lipid rafts, and cell membranes. Annu. Rev. Biophys. Biomol. Struct. *33*, 269–295.

Sorre, B., Callan-Jones, A., Manneville, J.B., Nassoy, P., Joanny, J.F., Prost, J., Goud, B., and Bassereau, P. (2009). Curvature-driven lipid sorting needs proximity to a demixing point and is aided by proteins. Proc. Natl. Acad. Sci. USA *106*, 5622–5626.

Souza, C.M., and Pichler, H. (2007). Lipid requirements for endocytosis in yeast. Biochim. Biophys. Acta *1771*, 442–454.

Tsai, B., Gilbert, J.M., Stehle, T., Lencer, W., Benjamin, T.L., and Rapoport, T.A. (2003). Gangliosides are receptors for murine polyoma virus and SV40. EMBO J. *22*, 4346–4355.

Windschiegl, B., and Steinem, C. (2006). Influence of alpha-hydroxylation of glycolipids on domain formation in lipid monolayers. Langmuir *22*, 7454–7457.

Windschiegl, B., Orth, A., Römer, W., Berland, L., Stechmann, B., Bassereau, P., Johannes, L., and Steinem, C. (2009). Lipid reorganization induced by Shiga toxin clustering on planar membranes. PLoS ONE *4*, e6238.

Zalevsky, J., Lempert, L., Kranitz, H., and Mullins, R.D. (2001). Different WASP family proteins stimulate different Arp2/3 complex-dependent actin-nucleating activities. Curr. Biol. *11*, 1903–1913.